




Article

Effectiveness of Road Cool Pavements, Greenery, and Canopies to Reduce the Urban Heat Island Effects

Paolo Peluso , Giovanni Persichetti  and Laura Moretti * 

Department of Civil, Constructional and Environmental Engineering, Sapienza University of Rome,
Via Eudossiana 18, 00184 Rome, Italy

* Correspondence: laura.moretti@uniroma1.it; Tel.: +39-06-44585114

Abstract: The ongoing climate change is manifesting itself through the increasing expansion of Urban Heat Island (UHI) effects. This paper evaluates the microclimate benefits due to cool road pavements, greenery, and photovoltaic canopies in a parking lot in Fondi (Italy), identifying the best strategy to counteract the negative effects of UHIs. The ENVI-met software allowed a microclimatic analysis of the examined area in July 2022 through the comparison of the thermal performances between the current asphalt pavement and ten alternative scenarios. The proposed layouts were investigated in terms of air temperature (AT), surface temperature (ST), mean radiant temperature (MRT), and predicted mean vote (PMV). The results showed that the existing asphalt pavement is the worst one, while the cool pavement integrated with vegetation provides appreciable benefits. Compared to the current layout, a new scenario characterized by light porous concrete for carriageable pavements and sidewalks, concrete grass grid pavers for parking stalls, a 2-m-high border hedge, and 15-m-high trees implies reductions of AT above 3 °C, ST above 30 °C, MRT above 20 °C, and a maximum PMV value equal to 2.2.

Keywords: urban heat islands; green furniture; cool pavements; photovoltaic canopies; predicted mean vote; thermal comfort



Citation: Peluso, P.; Persichetti, G.; Moretti, L. Effectiveness of Road Cool Pavements, Greenery, and Canopies to Reduce the Urban Heat Island Effects. *Sustainability* **2022**, *14*, 16027. <https://doi.org/10.3390/su142316027>

Academic Editor: Baojie He

Received: 2 November 2022

Accepted: 28 November 2022

Published: 30 November 2022

Publisher's Note: MDPI stays neutral with regard to jurisdictional claims in published maps and institutional affiliations.



Copyright: © 2022 by the authors. Licensee MDPI, Basel, Switzerland. This article is an open access article distributed under the terms and conditions of the Creative Commons Attribution (CC BY) license (<https://creativecommons.org/licenses/by/4.0/>).

1. Introduction

In the early 1800s, the meteorologist Howard [1–3] observed in London that the urban air temperature was higher than that of the surrounding areas. Over the decades, the economic and social opportunities of cities have attracted people from rural areas [4]. This phenomenon has contributed to reducing green and countryside areas and increasing facilities [5,6]. The anthropization factor caused the increase in air pollution and fostered the development of Urban Heat Islands (UHIs) [7,8]. In the last decades, the effects of the current global warming have exacerbated UHIs; new planning schemes are necessary to improve urban livability [9–11] with cost-effective measures. Indeed, urban artificial surfaces (e.g., roads, roofs, and buildings) over the day absorb solar radiation and store thermal energy; at night, heat energy is transferred to the atmosphere and causes a 1–3 °C air temperature increase [3,12]. This is enhanced by the summer diurnal temperatures and affects the physical and psychological discomfort of citizens [13]. Moreover, UHIs have a serious economic impact due to the energy consumption for cooling indoors [2,14].

According to [15,16], it is possible to counteract UHIs by means:

- light and permeable road pavements to improve the heat transmission between air and buildings;
- greenery and trees to realize urban green infrastructures (UGIs);
- sustainable transport and mobility to reduce the negative effects of private vehicles or conventional transport;
- evapotranspiration to decrease the heating of the local urban atmosphere;
- urban ventilation to improve the heat exchange.

A recent Italian standard provided for mandatory measures to counter UHIs, cool pavement materials, at least 60% permeable surfaces, and green furniture should be designed for all public parking works [17]. In this study, an existing parking lot in Fondi (Lazio, Italy) is modeled with the software ©2022 ENVI-met GmbH to gain its twin digital model. The survey area was chosen to conduct a preliminary assessment of the best sustainable redevelopment strategies for the site with a view towards future upgrades. The ENVI-Met software allows to recreate a real urban area and to evaluate its thermal conditions [18,19] through the return of reliable outputs in the real conditions [20,21]. After a validation procedure by comparing actual microclimate data with software output data, the current layout was modified with permeable light pavements and soft engineering solutions to investigate their effectiveness in mitigating UHI. This article proposes to replace the current layout of the studied area with 10 different scenarios based on recent cool pavement technologies. This study is a useful tool in order to evaluate which strategy appears to be the most appropriate to counteract the significant climate changes. The results expressed in terms of thermal and comfort parameters (i.e., AT, ST, MRT, and PMV) show quantitatively the interventions in an urban context that can ensure a high level of well-being.

2. Materials and Methods


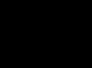






The increase in temperatures in urban areas is caused by the daytime thermal energy absorbed by artificial surfaces that is radiated during the night. This process is driven by both the albedo and emissivity of materials [3,14,15]. Albedo is the ratio between the reflected energy and the incident energy over a unit area [22]. It depends on: the material color and influences the surface temperature (ST), especially during the daytime [6,23,24], the wavelength of shortwave solar radiation, and the incident angles of variable direct solar radiation during the day [25]. Emissivity is the ratio between the energy radiated by an object compared to that radiated by a black body. It affects the surface temperatures of pavements, especially during the night [6,23,26]. In addition to the above two thermal properties, the conductivity (k) and thermal capacity (cp) also have an effect on the thermal response of an urban road pavement [23,27]. Thermal conductivity affects ST; the greater the thermal conductivity, the lower the daytime ST, and the opposite occurs at night. High cp values imply a reduction of the maximum ST, whereas low values favor the increase of the minimum ST [28,29]. However, k and cp cannot counteract UHI.

Therefore, the best two strategies are based on high albedo and emissivity building materials. The former relies on pavements with cool materials (e.g., limestone, light stone, and light concrete), the latter on permeable pavements to increase evapotranspiration and decrease the heating of the local urban atmosphere. Whatever the climate, cool materials could be effective, whereas porous pavements are suitable for warm temperate climates, such as in the studied parking lot. Three pavement materials were examined as an alternative to the existing asphalt:

- Porous light concrete has a 15–25% void structure. The high porosity gives mechanical strengths lower than those of traditional concrete and requires periodical cleaning to avoid pores' occlusion [30]. Large joint gaps between concrete blocks give permeable pavement as well [31].
- Concrete grass grid pavers allow both the evaporation of rainwater and evapotranspiration of grass. They are suitable for parking lots, because their use implies a low bearing capacity and high roughness [30,32].
- Stone pavers (e.g., limestone, basalt, and porphyry) are used in urban areas because of their aesthetic value. The blocks allow different layouts of the surfaces [33].

Table 1 synthesizes the pros and cons and the physical characteristics of the existing and the proposed building materials [34–36].

Table 1. Pros and cons of the examined building materials.

Material	Photo	Pros	Cons	Albedo	Emissivity	Color
Asphalt		Fast construction	UHI Low permeability	0.08	0.80	
Porous light concrete		Low surface temperature High albedo and emissivity values High permeability	Low strength High construction and maintenance costs Voids occlusion	0.80	0.94	
Concrete grass grid pavers		Evapotranspiration High permeability	Roughness Grass maintenance Noise	0.20	—	
Stone (porphyry)		Aesthetic value	Roughness Low albedo Noise	0.20	0.85	

The software © ENVI-met 5.0.3 was used for the microclimatic analysis, although it is not suitable for simulating an evaporative cooling effect of pervious pavements. Three input interfaces about the geometric, physical, and meteorological characteristics of the site permit processing three-dimensional (3D) simulation models. The results were analyzed with the Leonardo interface in terms of Air Temperature (AT), Surface temperature (ST), Mean Radiant Temperature (MRT), and Predicted Mean Vote (PMV) [37–39]. The PMV predicts people’s thermal comfort in steady-state conditions (Equation (1)). In this study, the reference man is 35 years old, 1.75 m tall, and weighs 75 kg [40,41]:

$$PMV = (0.303 \exp - 0.0336M + 0.028) \times \{(M - W) - 3.5 \times 10^{-3} \times [5733 - 6.99 \times (M - W) - p_a] - 0.42 \times (M - 58.5) - 1.7 \times 10^{-5} \times M \times (5867 - p_a) - 0.0014 \times M \times (34 - AT) - 3.96 \times 10^{-8} \times f_{cl} \times [(t_{cl} + 273)^4 - (t_r + 273)^4] - f_{cl} \times h_c \times (t_{cl} - AT)\} \quad (1)$$

where M is the metabolism rate, W is the external work, p_a is the partial water vapor pressure (Pa), f_{cl} is the surface area factor of clothing, t_{cl} is the surface temperature of clothing ($^{\circ}\text{C}$), h_c is the convective heat transfer coefficient ($\text{W}/(\text{m}^2 \times \text{K})$), AT is the air temperature ($^{\circ}\text{C}$), and t_r is the radiant temperature ($^{\circ}\text{C}$). Three different conditions are defined for the PMV according to the range of values assumed: ideal conditions (IC) for values between slightly cool (-1) and slightly warm ($+1$), acceptable conditions (AC) for values between ($-3, -1$) and ($1, 3$), and critical conditions (CC) for values over ± 3 .

The MRT quantifies the effect of environmental radiation on the human body. It depends on the surface’s emissivity and the shadows of the environment [42–45]. ENVI-met calculates the MRT according to Equation (2):

$$MRT^4 = \sum_{i=1}^N T_i^4 F_{p \rightarrow i} \quad (2)$$

where N is the number of the surrounding surfaces, T_i is the temperature of the i th surface, and $F_{p \rightarrow i}$ are the factors of view between the person and the whole surrounding environment.

The examined area is Archimede Rotunno Square in Fondi (Lazio, Italy; lat. $41^{\circ}21'12''$ –long. $13^{\circ}25'29''$). The model is composed of a grid of $40 \times 30 \times 30$ with a resolution of $2 \times 2 \times 2$ m (x, y, z). The model includes the central parking area (with six pink points that identify the receptors), an urban asphalt straight road on the right, two concrete buildings at the top and bottom of the image, and a green park on the left (Figure 1).

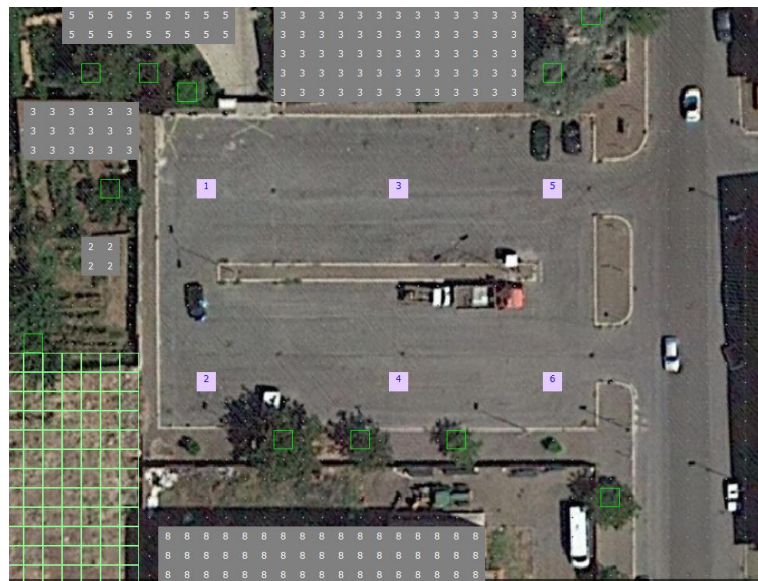


Figure 1. Archimede Rotunno Square in Fondi overlapped on the ENVI-Met.

The base model (S0) describes the current layout, with asphalt carriageable pavements and porphyry sidewalks (Figure 2). The rugged areas are sandy soil with albedo equal to 0.25 and emissivity equal to 0.90.

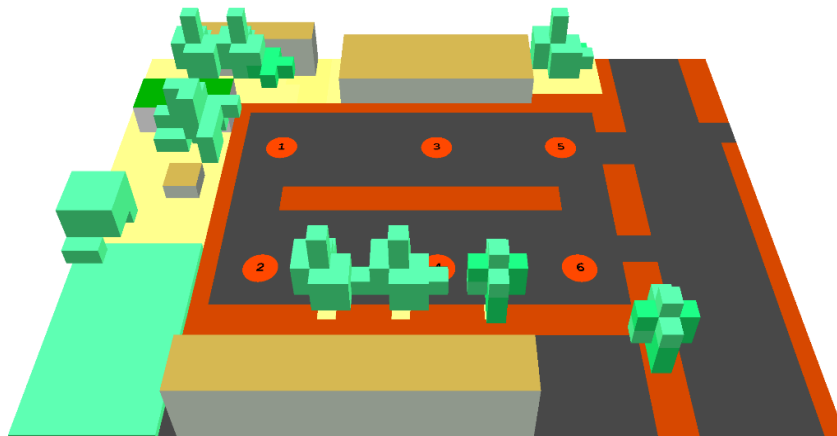


Figure 2. Three-dimensional model of the base model (S0).

Six receptors (1–6 pink and red points in Figures 1 and 2, respectively) were in the parking area to conduct the analysis. As performed in previous studies carried out by the authors [46], S0 was validated by comparing the AT calculated in the six receptors with those measured by the authors with the wi-fi weather station SBS-WS-500 Steinberg Systems (wind speed: 0–50 m/s, wind speed accuracy: $\pm 10\%$, humidity: 10–99%, humidity accuracy: $\pm 5\%$ (between 20% and 90%; 0–45 °C), and air temperature: -40 – $+60$ °C (outside), temperature accuracy: ± 1 °C). The comparison gave an average difference equal to 1.65 °C (the maximum value was 3.67 °C and the minimum one 0.08 °C). S0 presents the results in terms of the AT, MRT, and PMV consistent with the negative effects of UHIs; therefore, the authors propose to replace the current pavement with different layouts to improve microclimatic conditions (Table 2):

- Case 1.x focuses on the sidewalk's pavements; x ranges between 1 and 3, varying the sidewalk material;
- Case 2.x focuses on all the road pavements; x ranges between 1 and 3, varying the pavement material;

- Case 3.x focuses on all the road pavements and adds green furniture or photovoltaic panels to the area; x ranges between 1 and 4, varying the layout.

Table 2. Characteristics of the examined scenarios.

Scenario	Characteristics
S0	Asphalt carriageable pavements and porphyry pavers for sidewalks
S1.1	Asphalt carriageable pavements and concrete grass grid pavers for sidewalks
S1.2	Asphalt carriageable pavements and light porous concrete for sidewalks
S1.3	Asphalt carriageable pavements and grass for sidewalks
S2.1	Concrete grass grid pavers for carriageable pavements and sidewalks
S2.2	Light porous concrete for carriageable pavements and sidewalks
S2.3	Light porous concrete for carriageable pavements and sidewalks, and concrete grass grid pavers for stalls
S3.1	Light porous concrete for carriageable pavements and sidewalks, and concrete grass grid pavers for stalls + 2-m-high boundary hedge around the area + 11 5-m-high trees
S3.2	Light porous concrete for carriageable pavements and sidewalks, and concrete grass grid pavers for stalls + 2-m-high boundary hedge around the area + 43 5-m-high trees
S3.3	Light porous concrete for carriageable pavements and sidewalks, and concrete grass grid pavers for stalls + 2-m-high boundary hedge around the area + 43 15-m-high trees
S3.4	Light porous concrete for carriageable pavements and sidewalks, and concrete grass grid pavers for stalls + 2-m-high boundary hedge around the area + photovoltaic canopies over the parking stalls

The choice of the proposed scenarios and layouts aims to identify the best combination to mitigate the effects of UHIs. Scenarios S1.x and S2.x focus the microclimate investigation on the effects of sidewalks and pavement, respectively. Scenarios S3.x investigate the positive effects of the renewal of both the sidewalks and the lane with cool materials and also with the addition of green surfaces and photovoltaic panels, which can make parking management more sustainable.

The microclimate analysis was conducted in July 2022, as it is the most severe month [46]. The authors verified with a comparison with a 72-h simulation that a 48-h analysis is enough to reach numerical stability during the model spin-up phase (the maximum difference of PMV was 0.012, the maximum difference of AT was 0.097 °C, and the maximum difference of TMR was 0.155 °C). Therefore, a 48-h analysis was performed starting from 06.00 a.m. on 1 July 2022. Table 3 lists the meteorological input data [47].

Table 3. Meteorological input data.

Input Data	Value	Unit
Wind speed	2.00	m/s
Wind direction	90	°
Humidity at 2500 m	8	g/kg
Initial air temperature	23	°C
Maximum air temperature	30	°C
Initial humidity	70	%
Maximum humidity	75	%

For each receptor and scenario, the AT, ST, MRT, and PMV were assessed every six hours as of 12:00 a.m. on 2 July 2022 until 6:00 p.m. on 3 July 2022.

The main purpose of this study is to identify the layouts able to improve the environmental conditions and guarantee physical well-being and thermal comfort perceived by individuals, especially during the daytime.

3. Results

The Results section is divided into four subsections, one for each case examined. In this way, it is possible to interpret in detail the benefits resulting from a targeted intervention in the study area (i.e., sidewalks, road pavement, UGI, and canopies).

3.1. Current Scenario (S0)

Table 4 lists the results of S0 in terms of the PMV, AT, and MRT.

Table 4. Results of S0 in terms of the PMV, AT, and MRT.

Receptor	PMV (-)	AT (°C)	MRT (°C)	PMV (-)	AT (°C)	MRT (°C)	PMV (-)	AT (°C)	MRT (°C)	PMV (-)	AT (°C)	MRT (°C)
	12:00 a.m. 2 July			6:00 p.m. 2 July			00:00 a.m. 3 July			06:00 a.m. 3 July		
1	3.96	32.39	57.99	1.89	30.10	33.13	0.28	25.25	18.44	0.07	24.12	17.80
2	4.15	33.99	57.86	2.94	31.31	47.56	0.28	25.40	18.29	0.69	24.36	29.78
3	4.12	33.25	57.79	2.92	30.71	47.50	0.26	25.13	18.18	0.65	24.10	17.56
4	4.20	33.93	58.16	2.33	30.78	38.78	0.29	25.27	18.68	0.73	24.32	30.06
5	4.17	33.99	57.52	2.91	31.04	47.21	0.23	25.09	18.03	0.70	24.18	29.51
6	4.21	33.87	57.62	1.87	30.72	30.89	0.26	25.13	18.19	0.74	24.22	29.63

The daytime results highlight higher than 4 PMV values and higher than 57 °C MRT values that imply serious thermal stress and discomfort. However, the nighttime results are not critical: PMV is less than 0.7, and MRT and AT are about 18 °C and 25 °C, respectively. Figure 3a–d represents the AT, MRT, PMV, and ST map at 12.00 a.m. on 2 July, respectively.

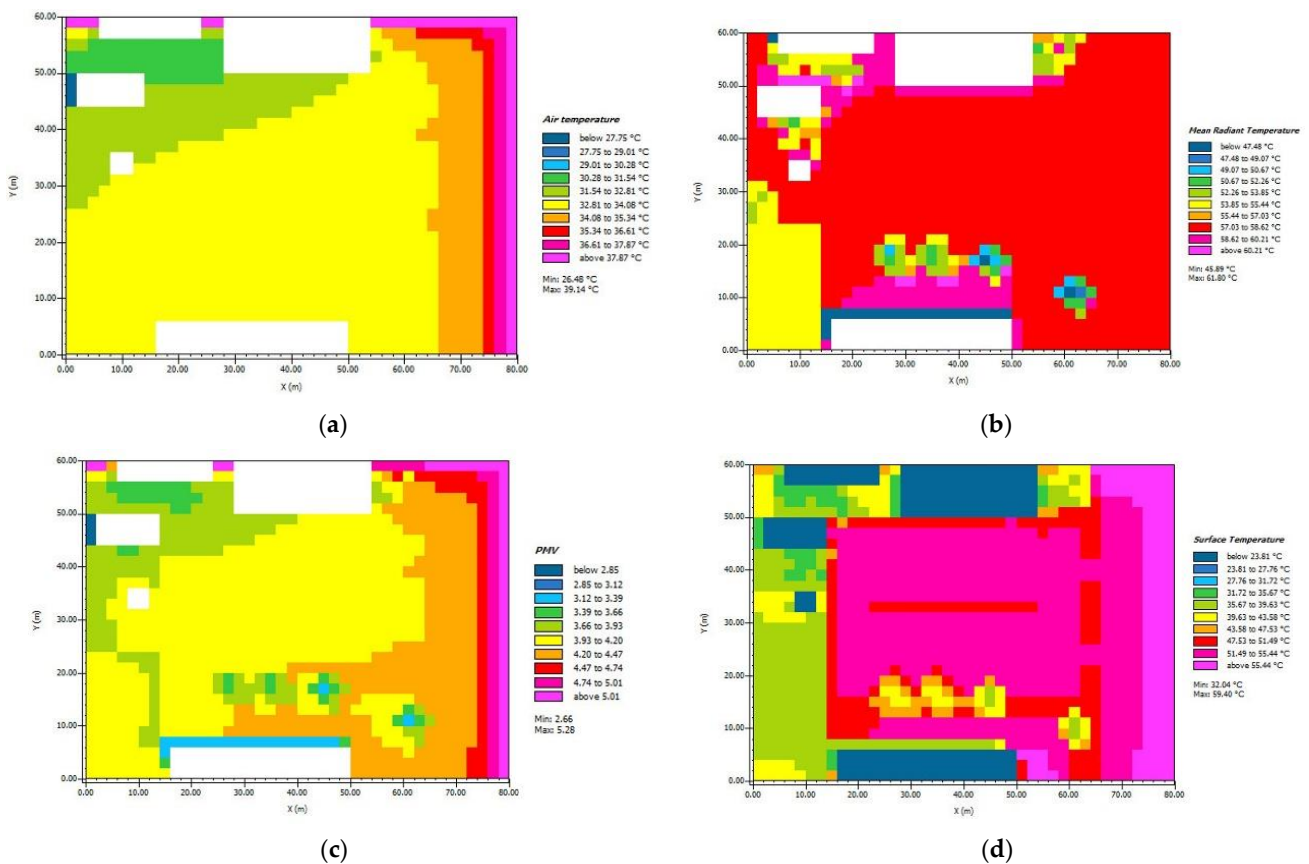


Figure 3. Leonardo maps of S0 at 12.00 a.m. on 2 July. (a) AT, (b) MRT, (c) PMV, and (d) ST.

The maps in Figure 3 show critical conditions for most of the modeled surfaces. Indeed, the existing black pavement absorbs a significant amount of heat, a direct consequence of the low albedo and high heat capacity of the asphalt-wearing layer [48].

3.2. Case 1.x

Case 1.x focuses its attention on the pedestrian surfaces surrounding the parking area. Porphyry pavers were substituted by concrete grass grid pavers (S1.1), light porous concrete (S1.2), and 5-cm-high grass (S1.3). Table 5 lists the results of Case 1.x in terms of the PMV, AT, and MRT.

Table 5. Results of Case 1.x in terms of the PMV, AT, and MRT.

Scenario	Receptor	PMV	AT	MRT	PMV	AT	MRT	PMV	AT	MRT	PMV	AT	MRT
		(-)	(°C)	(°C)	(-)	(°C)	(°C)	(-)	(°C)	(°C)	(-)	(°C)	(°C)
		12:00 a.m. 2 July			6:00 p.m. 2 July			00:00 a.m. 3 July			06:00 a.m. 3 July		
S1.1	1	3.89	31.51	60.69	1.67	29.12	32.30	0.07	24.53	16.88	-0.11	23.45	16.66
	2	4.12	32.70	60.55	2.68	29.97	47.03	0.04	24.46	16.74	0.49	23.47	29.04
	3	4.03	32.18	60.49	2.69	29.56	46.97	0.03	24.32	16.63	-0.13	23.35	16.43
	4	4.17	32.76	60.85	2.08	29.56	38.07	0.05	24.37	17.12	0.54	23.46	29.34
	5	4.14	32.72	60.17	2.65	29.72	46.66	0.00	24.20	16.49	0.51	23.33	28.80
	6	4.14	32.71	60.26	1.61	29.52	30.00	0.03	24.25	16.65	0.56	23.37	28.92
S1.2	1	3.92	31.51	61.39	1.68	29.13	32.41	0.07	24.52	16.85	-0.11	23.45	16.74
	2	4.17	32.73	61.25	2.68	29.96	47.13	0.03	24.44	16.71	0.49	23.46	29.11
	3	4.07	32.21	61.19	2.70	29.56	47.06	0.03	24.31	16.60	-0.12	23.34	16.51
	4	4.21	32.79	61.55	2.08	29.56	38.17	0.05	24.36	17.09	0.54	23.49	29.42
	5	4.17	32.73	60.87	2.65	29.71	46.75	-0.01	24.18	16.46	0.50	23.32	28.87
	6	4.17	32.71	60.96	1.61	29.51	30.11	0.02	24.24	16.61	0.55	23.36	28.99
S1.3	1	3.81	31.78	57.65	1.64	29.24	31.43	0.06	24.51	16.80	-0.12	23.46	16.46
	2	3.98	33.11	57.52	2.67	30.17	46.27	0.03	24.42	16.65	0.49	23.49	28.85
	3	3.96	32.52	57.46	2.66	29.71	46.20	0.03	24.29	16.54	-0.13	23.36	16.23
	4	4.03	33.08	57.82	2.05	29.69	37.24	0.04	24.34	17.03	0.54	23.48	29.17
	5	4.02	33.22	57.18	2.64	29.92	45.90	-0.01	24.15	16.40	0.51	23.35	28.62
	6	4.07	33.11	57.27	1.58	29.64	29.13	0.02	24.24	16.56	0.55	23.39	28.74

Whatever the hour, the PMV results do not differ significantly between the scenarios of Case 1.x (the minimum value is 3.89, 3.92, and 3.81 in S1.1–S1.3, respectively). Low differences are between S0 and Case 1.x over the nighttime (the average value of the PMV is 0.27 in S0, 0.04 in S1.1, and 0.03 in S1.2 and S1.3). Regarding AT, at 12.00 on 2 July, the AT ranges between 31.51 °C of S1.1 and 33.22 °C of S1.3. S1.1 and S1.2 during the daytime have a similar trend that is better than S0 (at 12.00, AT in S0 ranges between 32.39 °C and 33.99 °C). At 12.00 a.m., both the grass grid pavers in S1.1 and the porous concrete in S1.2 imply a 1 °C AT reduction compared to S0 (the average AT values are 32.43 °C and 32.45, respectively, against 33.57 °C of S0). It should be noted that the software does not allow simulations of the evaporative cooling effect of pervious pavements; the results are worse than they should be. S1.3 gives slightly worse results (the average AT is 32.80 °C). At midday, the MRT assumes high values both in S0 and Case 1.x (the minimum value is 57.52 °C in S0, 60.17 °C, 60.87 °C, and 57.18 °C in S1.1–S1.3, respectively). S1.1 and S1.2 give the worse results than S0, while S1.3 shows small improvements due to the sidewalk's grass. During the nighttime, both S0 and Case 1.x have absolute low values whose trends are comparable to the daytime results.

Figure 4a–d shows the PMV map of S0 and S1.1–S1.3, respectively, at 12.00 a.m. on 2 July.

At midday, the minimum and maximum PMV values of Case 1.x range between 2.72 and 5.03 of S1.1, 2.76 and 5.06 of S1.2, and 2.58 and 4.99 of S1.3. This last scenario ensures the best performance compared to S0, whose minimum and maximum PMV values are 2.66 and 5.28, respectively. The results highlight that replacing porphyry sidewalks with

porous concrete pavements or concrete grass grid pavers brings about a negligible benefit. The small extension of the modified surface justifies these results.

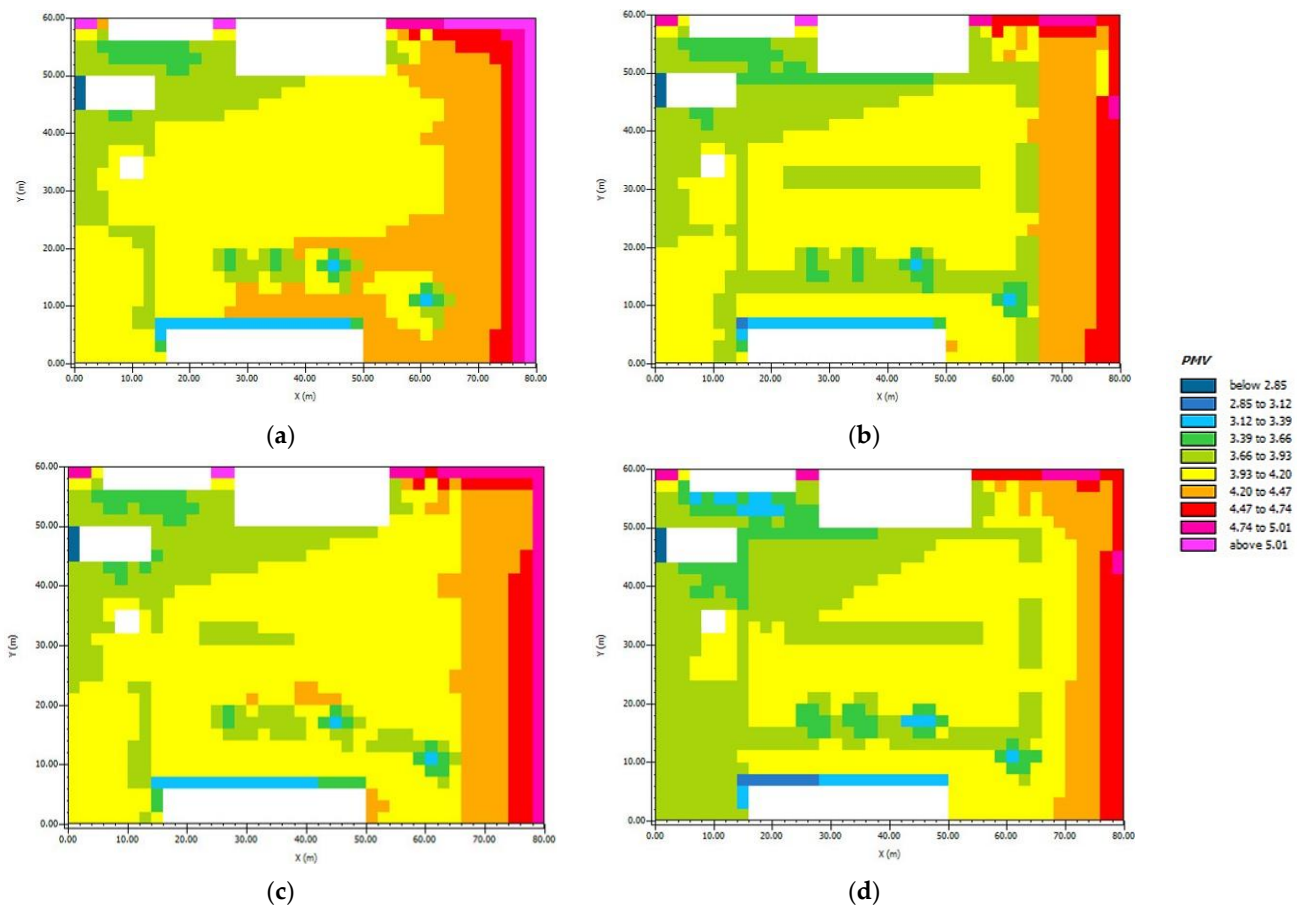


Figure 4. PMV map at 12.00 a.m. on 2 July. (a) S0, (b) S1.1, (c) S1.2, and (d) S1.3.

3.3. Case 2.x

Case 2.x modifies both sidewalk and parking pavements. Concrete grass grid pavers and porous light concrete are the overall pavements in S2.1 and S2.2, respectively. S2.3 has concrete grass grid pavers for stalls and porous light concrete for the other road surfaces. Table 6 lists the results of Case 2.x in terms of the PMV, AT, and MRT.

The best technical and environmental scenario is S2.3. Indeed, during the daytime, road materials with high albedo and emissivity contribute to reducing both the AT and PMV compared to S0 (average reduction of 0.88 °C and 0.37, respectively); at 6.00 p.m. on 2 July PMV is near the comfort zone (i.e., 2.15). Nevertheless, the average MRT value is high both at 12.00 a.m. and 6.00 p.m. (54.54 °C and 37.88 °C, respectively). Figure 5a–d shows the PMV map of S0 and S2.1–S2.3, respectively, at 12.00 on 2 July.

S2.1 has the best PMV values of Case 2.x (the average PMV is 3.61 at 12.00 on 2 July). From an environmental perspective, S2.1 is the most suitable option, but concrete grass grids make up a discontinuous pavement, resulting in discomfort for pedestrians or light vehicles. Therefore, S2.3 is preferred, because its average PMV is 3.76 at 12.00 on 2 July compared to 3.91 of S2.2.

Case 2.x partly transposes [17], because all the road surfaces are permeable and cool. The results are better than Case 1.x, but they are not enough to guarantee a favorable state of comfort or to mitigate the UHI.

Table 6. Results of Case 2.x in terms of the PMV, AT, and MRT.

Scenario	Receptor	PMV	AT	MRT	PMV	AT	MRT	PMV	AT	MRT	PMV	AT	MRT
		(-)	(°C)	(°C)	(-)	(°C)	(°C)	(-)	(°C)	(°C)	(-)	(°C)	(°C)
		12:00 a.m. 2 July			6:00 p.m. 2 July			00:00 a.m. 3 July			06:00 a.m. 3 July		
S2.1	1	3.44	31.41	52.61	1.69	29.55	31.21	0.19	24.75	18.26	-0.04	23.59	17.38
	2	3.57	32.59	52.54	2.23	30.46	38.09	0.17	24.75	18.18	0.11	23.60	20.67
	3	3.59	32.20	52.46	2.20	30.01	38.00	0.16	24.58	18.07	-0.05	23.49	17.20
	4	3.65	32.69	52.80	2.01	30.12	35.10	0.18	24.65	18.52	0.14	23.56	20.97
	5	3.68	33.10	52.32	2.21	30.35	37.84	0.13	24.47	18.04	0.11	23.47	20.53
	6	3.70	32.93	52.39	1.66	30.10	29.04	0.15	24.49	18.17	0.14	23.49	20.60
S2.2	1	3.75	31.76	56.61	1.74	29.62	32.01	0.13	24.74	17.27	-0.09	23.58	16.61
	2	3.89	33.10	56.49	2.77	30.61	30.06	0.10	24.72	17.13	0.51	23.62	28.96
	3	3.90	32.54	56.42	2.76	30.12	46.66	0.09	24.55	17.02	-0.11	23.49	16.37
	4	3.96	33.08	56.78	2.15	30.11	37.77	0.11	24.61	17.51	0.56	23.58	29.27
	5	3.95	33.29	56.16	2.74	30.38	46.37	0.06	24.43	16.88	0.52	23.48	28.73
	6	3.98	33.13	56.25	1.69	30.06	29.74	0.08	24.46	17.04	0.57	23.50	28.85
S2.3	1	3.70	31.57	56.42	1.74	29.59	32.00	0.13	24.75	17.33	-0.08	23.59	16.62
	2	3.64	32.91	52.79	2.24	30.58	38.10	0.16	24.74	18.12	0.10	23.61	20.65
	3	3.87	32.38	56.23	2.77	30.09	46.65	0.10	24.56	17.07	-0.10	23.49	16.39
	4	3.70	32.96	53.05	2.01	30.17	35.10	0.17	24.63	18.46	0.13	23.58	20.95
	5	3.94	33.23	56.01	2.75	30.39	46.40	0.07	24.45	16.96	0.54	23.48	28.76
	6	3.73	33.08	52.63	1.65	30.10	29.03	0.14	24.48	18.10	0.13	23.49	20.60

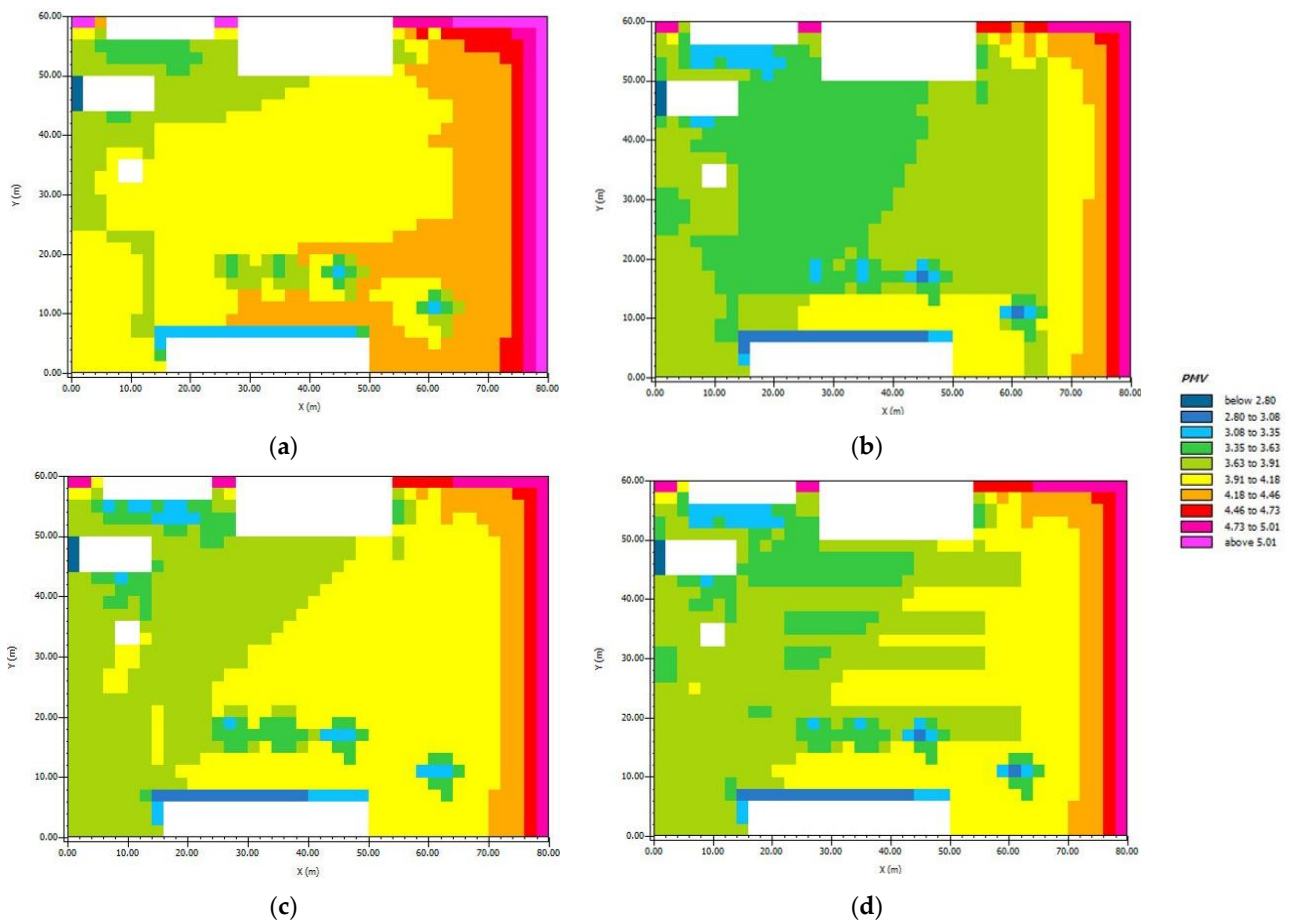


Figure 5. PMV map at 12.00 a.m. on 2 July. (a) S0, (b) S2.1, (c) S2.2, and (d) S2.3.

3.4. Case 3.x

Case 3.x fully transposes [17], because it adds green coverage for at least 10% of the gross parking area, not less than a 1-m-high boundary hedge, and any photovoltaic canopies above the stalls. Figure 6a–d represents the layout of S3.1–S3.4, respectively.

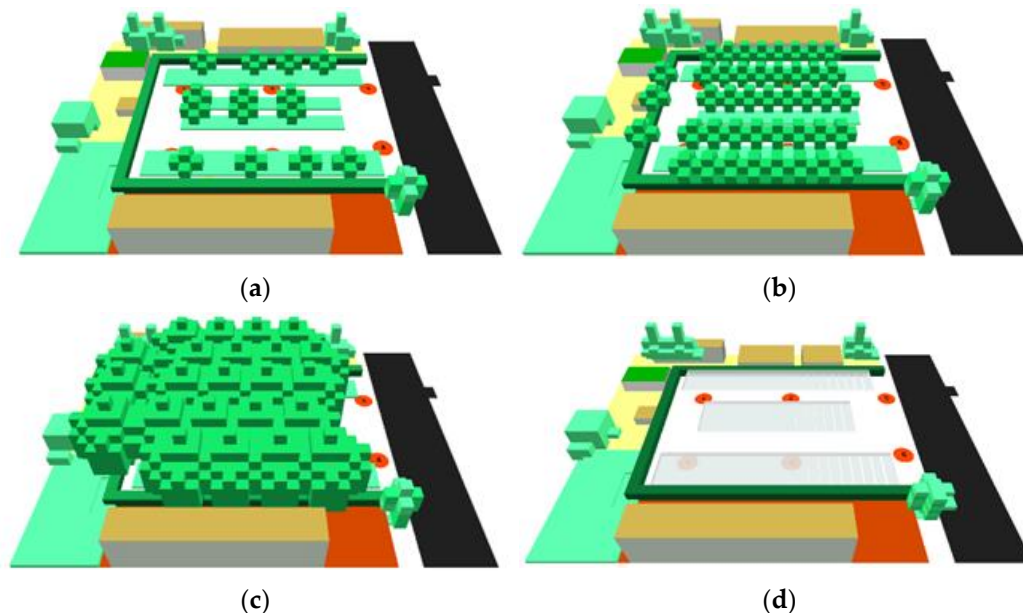


Figure 6. ENVI-met models. (a) S3.1, (b) S3.2, (c) S3.3, and (d) S3.4.

Table 7 lists the results of Case 3.x in terms of the PMV, AT, and MRT.

Table 7. Results of Case 3.x in terms of the PMV, AT, and MRT.

Scenario	Receptor	PMV	AT	MRT	PMV	AT	MRT	PMV	AT	MRT	PMV	AT	MRT
		(-)	(°C)	(°C)	(-)	(°C)	(°C)	(-)	(°C)	(°C)	(-)	(°C)	(°C)
		12:00 a.m. 2 July			6:00 p.m. 2 July			00:00 a.m. 3 July			06:00 a.m. 3 July		
S3.1	1	3.63	31.44	55.48	2.71	29.64	46.28	0.13	24.75	17.33	-0.08	23.59	16.62
	2	3.61	32.84	51.82	2.21	30.41	37.54	0.16	24.74	18.12	0.10	23.61	20.65
	3	3.83	32.35	55.53	2.77	29.93	46.34	0.10	24.56	17.07	-0.10	23.49	16.39
	4	3.63	33.01	51.96	1.62	30.01	28.78	0.17	24.63	18.46	0.13	23.58	20.95
	5	3.87	33.04	55.12	2.69	30.14	45.84	0.07	24.45	16.96	0.54	23.48	28.76
	6	3.66	32.95	51.93	1.60	29.87	28.72	0.14	24.48	18.10	0.13	23.49	20.60
S3.2	1	3.02	30.48	47.01	1.71	29.08	31.67	0.59	25.12	23.32	0.34	23.94	22.00
	2	3.51	31.84	51.32	2.26	29.98	38.05	0.43	25.15	20.88	0.18	23.90	19.61
	3	3.21	31.39	47.65	1.76	29.17	32.47	0.60	24.85	24.45	0.36	23.77	23.01
	4	3.63	32.36	51.97	2.24	29.77	38.85	0.43	24.87	22.02	0.19	23.76	20.64
	5	3.79	32.89	53.61	1.49	29.67	27.37	0.17	24.56	17.49	0.65	23.57	29.66
	6	3.53	32.86	50.32	2.10	29.91	36.83	0.22	24.57	19.17	0.19	23.57	21.40
S3.3	1	1.87	28.52	35.59	1.20	27.60	27.96	0.47	24.82	23.03	0.25	23.82	21.82
	2	1.99	29.40	35.08	1.25	27.90	27.87	0.49	24.82	23.11	0.27	23.79	21.89
	3	1.97	29.41	35.41	1.18	27.68	27.75	0.40	24.56	22.87	0.19	23.64	21.65
	4	2.05	30.22	34.87	1.19	27.90	27.69	0.38	24.55	22.97	0.17	23.63	21.75
	5	2.63	31.71	40.20	1.20	28.08	27.15	0.29	24.36	21.56	0.78	23.53	32.56
	6	3.02	32.10	45.66	1.22	28.17	27.38	0.30	24.36	21.98	0.29	23.53	24.19
S3.4	1	3.00	29.23	52.21	2.15	27.77	44.00	0.03	24.60	15.92	-0.13	23.62	15.67
	2	2.22	29.47	40.16	1.14	27.90	26.82	-0.01	24.68	14.88	-0.15	23.67	15.34
	3	3.03	29.45	52.23	2.15	27.81	43.94	-0.01	24.48	15.49	-0.16	23.55	15.37
	4	2.27	29.69	40.04	1.14	27.94	26.68	-0.04	24.55	14.57	-0.17	23.60	15.08
	5	3.17	30.31	52.13	2.18	28.01	43.85	-0.03	24.23	15.74	0.48	23.41	27.93
	6	2.42	30.47	39.39	1.18	28.13	26.62	-0.07	24.30	14.70	0.49	23.46	27.62

The green furniture in S3.3 guarantees thermal comfort, because the average PMV decreases to 2.25 at 12.00 a.m. and 1.21 at 6.00 p.m. The photovoltaic canopies in S3.4 shadow the area, reducing the ST and leading to an average PMV value of 2.68 at 12.00 a.m. According to Tables 6 and 7, at night, there is a slight deterioration in terms of the AT and PMV, because the trees are a barrier and retain the heat of the day under their foliage. At 00.00 a.m. and 6.00 a.m., S3.4 is the best solution (the average AT is 24.47 °C and 23.55 °C, respectively, against 24.58 °C and 23.65 °C of S3.3). The average PMV is almost neutral, equal to -0.02 and 0.06 , respectively, against 0.39 and 0.33 of S3.3). However, the trees contribute to the drastic diurnal reduction of MRT; the average MRT at 12.00 a.m. on 2 July reaches 57.82 °C in S0, while it is 53.64 °C in S3.1, 50.31 °C in S3.2, and 37.80 °C in S3.3. Overall, the daytime benefits of trees far outweigh the disadvantages of the nighttime hours. The average MRT value of 3.4 at 12.00 a.m. is 46.02 °C; the performance of the layout with canopies is intermediate between the current scenario and those with green furniture.

Figure 7a–d shows the PMV absolute difference between S0 and S3.1–S3.4, respectively, at 12.00 on 2 July.

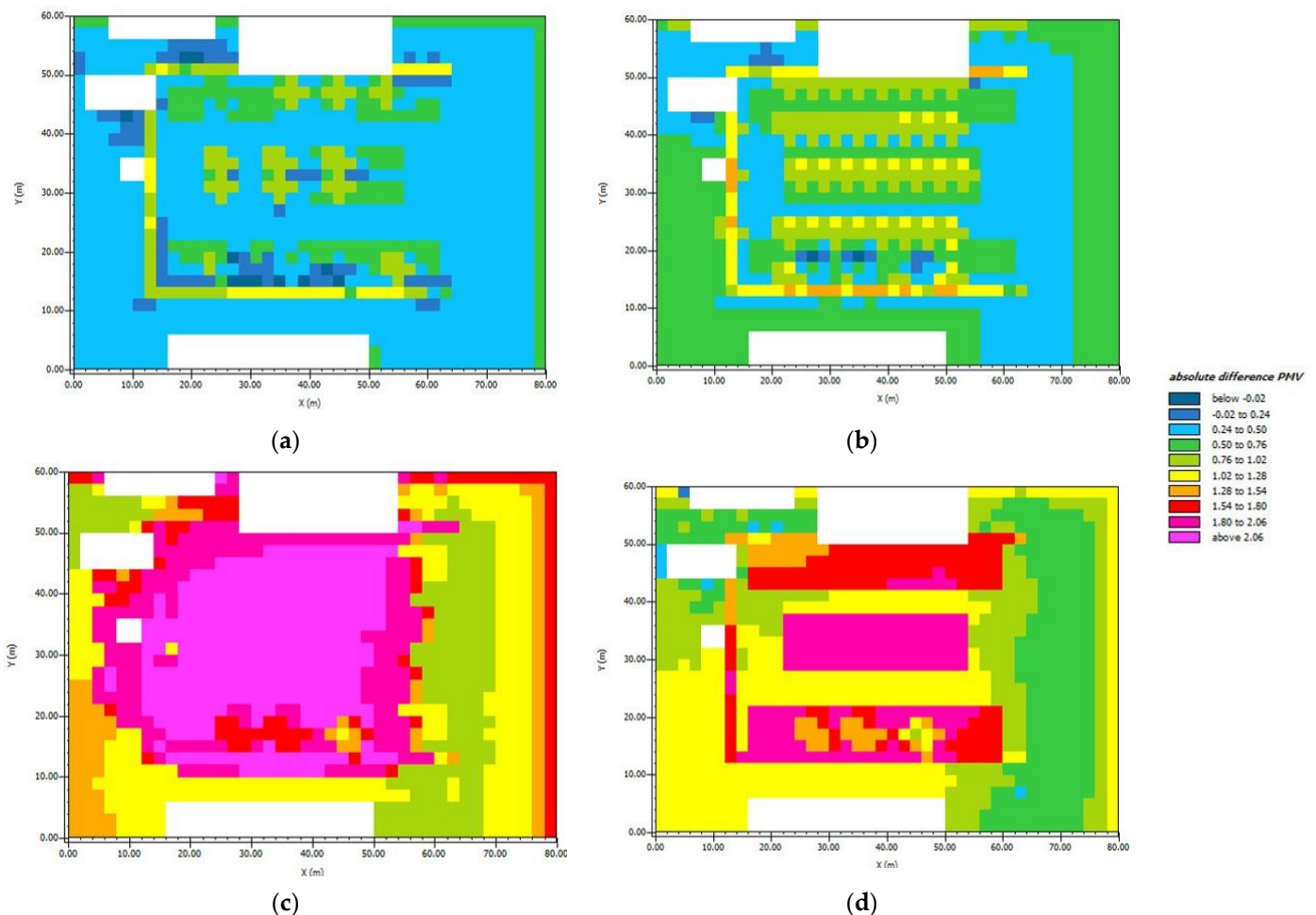


Figure 7. The PMV absolute difference map at 12.00 a.m. on 2 July between S0 and (a) S3.1, (b) S3.2, (c) S3.3, and (d) S3.4.

At 12:00 a.m., S3.1 and S3.2 give similar PMV results compared to S0 (Figure 7a,b); the average absolute difference is 0.42 and 0.68, respectively. On the other hand, S3.3 gives the highest absolute difference PMV (i.e., above 1.8).

Figure 8a–d shows the absolute difference between MRT in S0 and S3.1–S3.4, respectively, at 12.00 on 2 July.

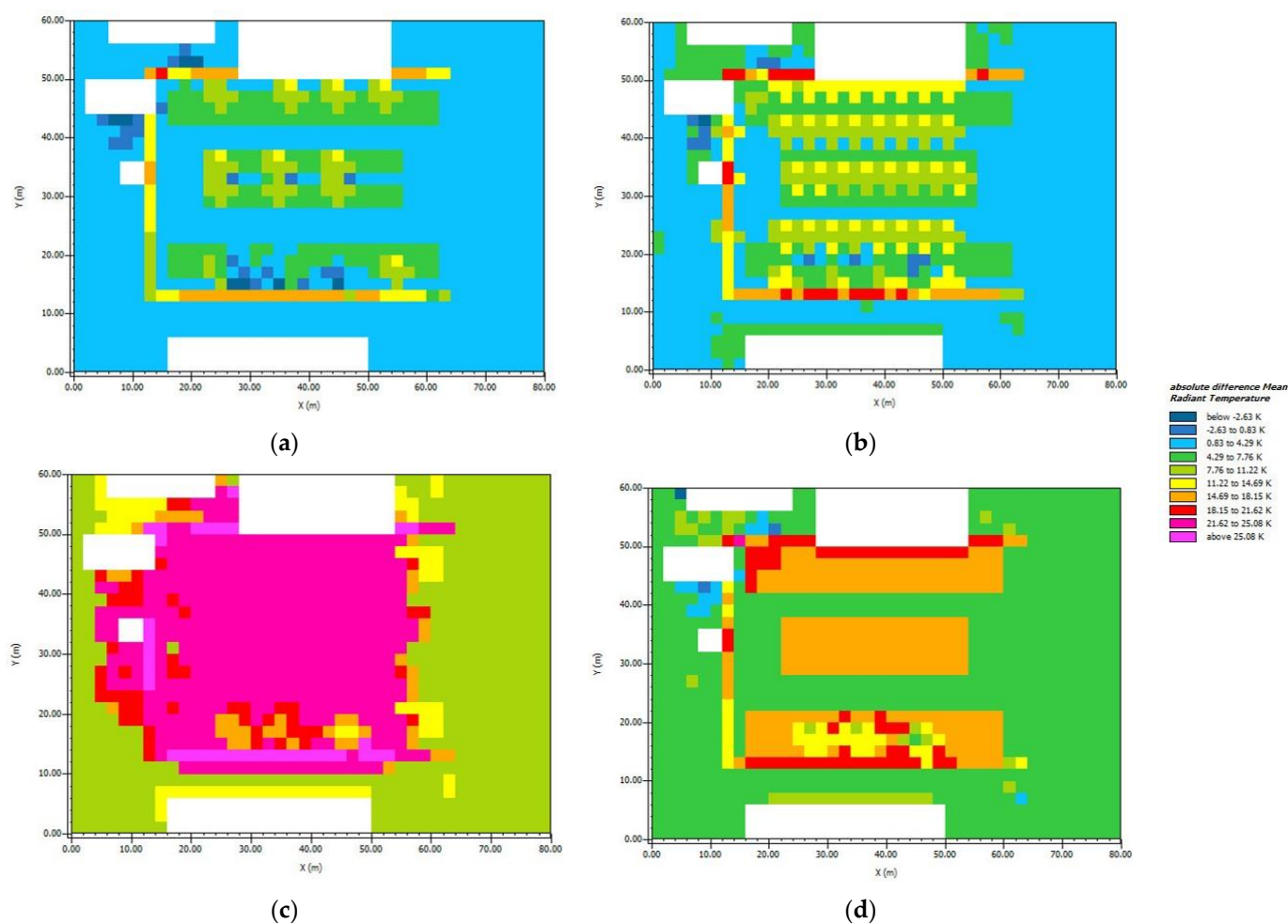


Figure 8. The MRT absolute difference map at 12.00 a.m. on 2 July between S0 and (a) S3.1, (b) S3.2, (c) S3.3, and (d) S3.4.

The results confirm studies in the literature where dense and strategically arranged trees reduced the MRT, especially in open sites [49] and canopy shade and reduced the direct radiation, offering benefits against heat stress [50]. Figure 9a–d represents ST maps of S0, S2.3, S3.3, and S3.4, respectively, at 12.00 on 2 July.

The ST maps in Figure 9 highlight the pivotal role of trees and shade to reduce ST. At midday, in S0, the maximum ST value is 59.4 °C (Figure 9a), whereas it is 55.61 °C, 52.23 °C, and 52.57 °C in S2.3, S3.3, and S3.4, respectively. In particular, the presence of shaded areas is also beneficial for the surrounding areas, as confirmed by the ST trend of the road on the east side of the model.

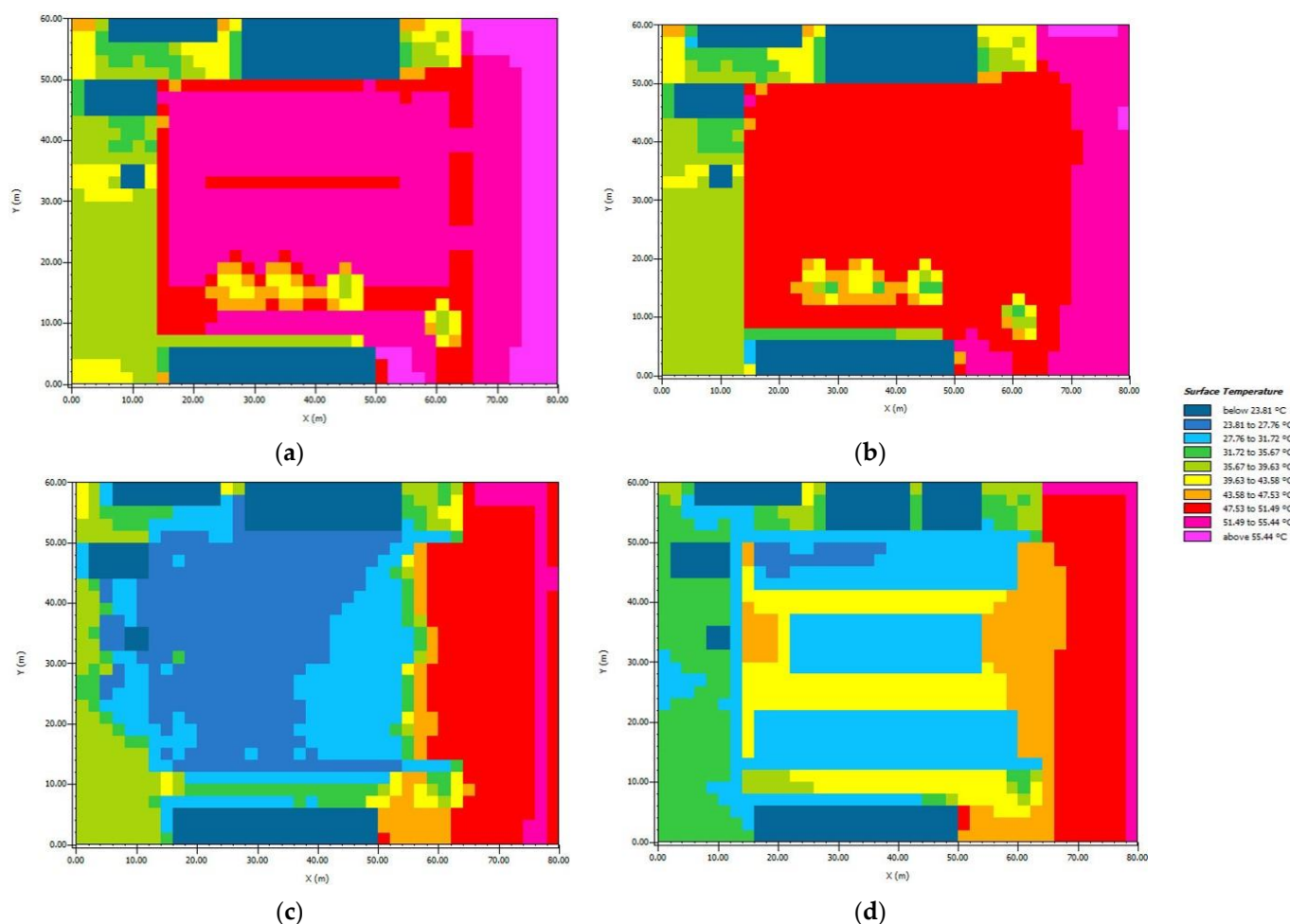


Figure 9. ST map at 12.00 a.m. on 2 July. (a) S0, (b) S2.3, (c) S3.3, and (d) S3.4.

4. Discussion

In this manuscript, the authors proposed an application of recent innovations in UHI mitigation to a real case of study. In detail, the area examined was a parking lot in the City of Fondi (Lazio, Italy). The implementation of the current parking lot conditions in ENVI-Met software demonstrated the presence of adverse microclimatic conditions. Therefore, in this study, several useful scenarios were proposed to foster and ensure better living conditions for humans. They differed from each other in the gradual replacement of the current conditions, so that improvements from the introduction of a particular cool strategy could be read in detail. The results were analyzed in terms of the AT, MRT, ST, and PMV and demonstrated in accordance with the scientific literature the benign effects associated with the introduction of cool material and UGIs [51–53].

Figures 7–9 demonstrate that S3.3 gives satisfactory results, because it is possible to achieve the objectives of reducing temperatures and ensuring PMV in the comfort zone during the daytime. Moreover, this solution is sustainable due to the presence of large trees and permeable road pavements [54]. According to recent studies, this article enhances the cooling performance of permeable pavements [55,56] and green furniture in an urban context [57,58]. Conversely, the absence of trees in S3.4 turns the alternative less “green” but qualifies the proposed scenario as the best option from an energy point of view. Indeed, the produced electricity can be used to recharge electric or plug-in hybrid vehicles. Therefore, the authors conducted the energy analysis of S3.4 based on the following assumptions:

- On average, 7.2 m² of solar cells are necessary to build a 1-kW power plant if they are correctly positioned and tilted. In S3.4, the cells were horizontal; thus, the efficiency of energy production was reduced by a factor of 0.75 [59];

- A factor of 0.8 takes into account the system losses [60];
- The overall cell surface is 1500 m².

According to [61], the annual solar radiation on the horizontal plane for Latina, a city near Fondi, is 1673 kWh/m². Therefore, according to [62], it is possible to value the theoretical annual gain *G* of the plant, which is equal to 20,326.95 kWh. Since an electric car consumes, on average, 15 kWh/100 km [63], the energy produced by the photovoltaic canopies is enough to travel 120,906 km/year. Since 60 stalls are in the parking area, each car parked during the year can recharge its batteries and travel about 2000 km. Therefore, S3.4 would create new favorable solutions for the Italian energy market to reduce the dependence on fossil fuels and promote carbon-neutral mobility.

The analysis focused on physical (air temperature, surface temperature, and mean radiant temperature) and thermal–physiological (predicted mean vote) variables, but structural issues cannot be overlooked [64,65]. The results showed that the thermophysical properties of building materials play a pivotal role in improving the quality of life. Finally, even during the hottest hours, the inclusion of UGIs and photovoltaic canopies boosted the benefits of cool pavement, favoring the reduction of thermal parameters and increasing human comfort.

5. Conclusions

Traditional black and low-permeable road asphalt pavements contribute to UHIs, because the wearing material has low albedo and emissivity and a high thermal capacity. They overheat and absorb heat from the sun in the daytime and radiate it out as the temperature drops. The negative thermophysical effects overlap with those from climate change and require mitigation strategies. Cool materials and green furniture improve livability in the urban environment, because they reduce both the ST and AT and allow evapotranspiration.

With ENVI-Met, a 3D twin digital model of a parking lot in Fondi (Lazio, Italy) was modeled. According to the Italian Ministry of the Environment (2017), the current low-permeable pavement was replaced with a permeable one and green furniture was added in ten alternative scenarios. The microclimate of the examined area was described by the air temperature, surface temperature, mean radiant temperature, and PMV in the hottest month of the year. The results showed that the best scenarios from a technical–environmental point of view have pavements composed of grass concrete grids and light permeable concrete, respectively, for parking stalls and carriageable areas. Indeed, high albedo and emissivity reduce the AT (e.g., at 12.00 a.m. AT is 32.69 °C in S2.3 compared to 33.57 °C in S0) and ensure thermal comfort (at 12.00 a.m. PMV is 3.76 in S2.3 compared to 4.13 S0), but they are not enough to counteract the effects of UHIs. Therefore, green furniture composed of trees and hedges has been added to the area; they shade surfaces, reducing at 12.00 a.m. both the AT (there is a difference of over 3 °C between S3.3 and Case S0 at 30.23 °C vs. 33.57 °C) and MRT (37.80 °C of S3.3 vs. 57.82 °C of S0). S3.3 is the best scenario, as the main objective (i.e., mitigation of the heat island in the hottest hours) is achieved with soft engineering strategies (i.e., greenery and permeable pavements) that are compliant with the current Italian standards. Finally, a scenario with photovoltaic shelters covering the parking stalls was modeled (S3.4). The thermal and environmental results were appreciable during the day (at 12.00, the PMV and AT were 2.68 and 29.77 °C, respectively, compared to 4.13 and 33.57 °C of S0). Case 3.4 not only shows thermal and comfort benefits but also foreshadows the benefits associated with this strategy. The incorporation of photovoltaic canopies in the parking area enables sustainable power generation for public destinations and answers the rapid growth in e-mobility.

The results showed the great benefits from the implementation of the strategies proposed to counteract and mitigate the effects of UHIs. The use of cool pavements, greenery and canopies returned appreciable results in urban public spaces whose redesigns can ensure a better quality of life. This case study is a useful tool to identify the best technology to oppose UHIs and extend the chosen methodology to other real-world cases. In the future,

further studies will be carried out to improve the proposed technologies and identify even more efficient solutions to slow climate change and environmental degradation.

Author Contributions: Conceptualization, P.P., G.P. and L.M.; Formal analysis, G.P. and L.M.; Methodology, G.P.; Software, P.P. and G.P.; Validation, P.P. and L.M.; Visualization, P.P.; Writing—original draft, G.P. and L.M.; and Writing—review and editing, P.P. and L.M. All authors have read and agreed to the published version of the manuscript.

Funding: This research received no external funding.

Institutional Review Board Statement: Not applicable.

Informed Consent Statement: Not applicable.

Data Availability Statement: The data presented in this study are available on request from the corresponding author. The data are not publicly available due to confidentiality reasons.

Conflicts of Interest: The authors declare no conflict of interest.

References

- Oke, T. The Energetic Basis of the Urban Heat Island. *Q. J. R. Meteorol. Soc.* **1982**, *108*, 1–24. [\[CrossRef\]](#)
- Miner, M.J.; Taylor, R.A.; Jones, C.; Phelan, P.E. Efficiency, Economics, and the Urban Heat Island. *Environ. Urban.* **2017**, *29*, 183–194. [\[CrossRef\]](#)
- Weng, Q.; Quattrocchi, D.A. (Eds.) *Urban Remote Sensing*; CRC Press: Boca Raton, FL, USA, 2006; ISBN 9781315166612.
- Hoogerbrugge, M.M.; Burger, M.J. Selective Migration and Urban–Rural Differences in Subjective Well-Being: Evidence from the United Kingdom. *Urban Stud.* **2022**, *59*, 2092–2109. [\[CrossRef\]](#)
- Li, F.; Zheng, W.; Wang, Y.; Liang, J.; Xie, S.; Guo, S.; Li, X.; Yu, C. Urban Green Space Fragmentation and Urbanization: A Spatiotemporal Perspective. *Forests* **2019**, *10*, 333. [\[CrossRef\]](#)
- Dekić, J.P.; Mitković, P.B.; Dinic Branković, M.M.; Igić, M.Z.; Dekić, P.S.; Mitković, M.P. The Study of Effects of Greenery on Temperature Reduction in Urban Areas. *Therm. Sci.* **2018**, *22*, 988–1000. [\[CrossRef\]](#)
- Halder, B.; Bandyopadhyay, J.; Khedher, K.M.; Fai, C.M.; Tangang, F.; Yaseen, Z.M. Delineation of Urban Expansion Influences Urban Heat Islands and Natural Environment Using Remote Sensing and GIS-Based in Industrial Area. *Environ. Sci. Pollut. Res.* **2022**, *29*, 73147–73170. [\[CrossRef\]](#)
- Mohajerani, A.; Bakaric, J.; Jeffrey-Bailey, T. The Urban Heat Island Effect, Its Causes, and Mitigation, with Reference to the Thermal Properties of Asphalt Concrete. *J. Environ. Manag.* **2017**, *197*, 522–538. [\[CrossRef\]](#)
- Akbari, H.; Kolokotsa, D. Three Decades of Urban Heat Islands and Mitigation Technologies Research. *Energy Build.* **2016**, *133*, 834–842. [\[CrossRef\]](#)
- Anupam, B.R.; Chandrappa, A.K.; Sahoo, U.C. Sustainable Pavements for Low-Impact Developments in Urban Localities. In *Advances in Sustainable Materials and Resilient Infrastructure*; Springer: Singapore, 2022; pp. 159–184. [\[CrossRef\]](#)
- Ranieri, V.; Coropulis, S.; Berloco, N.; Fedele, V.; Intini, P.; Laricchia, C.; Colonna, P. The Effect of Different Road Pavement Typologies on Urban Heat Island: A Case Study. *Sustain. Resilient Infrastruct.* **2022**, *7*, 1–20. [\[CrossRef\]](#)
- Cantelli, A.; Monti, P.; Leuzzi, G. Influence of the Urban Heat Island Parameterization on Precipitation Forecasting in Limited Area Model. In *Environmental Hydraulics*; CRC Press: Boca Raton, FL, USA, 2010; Volume 2, pp. 1151–1156. [\[CrossRef\]](#)
- de Martino, A.; Vasselli, S.; D’Argenio, P. Strategies for protecting the elderly from the health-risks of heat-waves: Measures undertaken in Italy in the summer of 2004. *Ig. Sanita Pubblica* **2005**, *61*, 293–312.
- Santamouris, M. Using Cool Pavements as a Mitigation Strategy to Fight Urban Heat Island—A Review of the Actual Developments. *Renew. Sustain. Energy Rev.* **2013**, *26*, 224–240. [\[CrossRef\]](#)
- Musco, F.; Fregolent, L.; Magni, F.; Maragno, D.; Ferro, D. *Calmierare gli Impatti del Fenomeno Delle Isole di Calore Urbano Con la Pianificazione Urbanistica: Esiti e Applicazioni del Progetto Uhi (Central Europe) in Veneto*; Ispra: Rome, Italy, 2014; ISBN 9788844806866.
- Shahmohamadi, P.; Cubasch, U.; Sodoudi, S.; Che-Ani, A.I. Mitigating Urban Heat Island Effects in Tehran Metropolitan Area. In *Air Pollution—A Comprehensive Perspective*; Haryanto, B., Ed.; IntechOpen: London, UK, 2012. [\[CrossRef\]](#)
- Italian Ministry of the Environment. *Adozione Dei Criteri Ambientali Minimi per l’Affidamento di Servizi di Progettazione e Lavori per la Nuova Costruzione, Ristrutturazione e Manutenzione di Edifici Pubblici*; Italian Ministry of the Environment: Rome, Italy, 2017.
- Alves, F.M.; Gonçalves, A.; del Caz-Enjuto, M.R. The Use of Envi-Met for the Assessment of Nature-Based Solutions’ Potential Benefits in Industrial Parks—A Case Study of Argales Industrial Park (Valladolid, Spain). *Infrastructures* **2022**, *7*, 85. [\[CrossRef\]](#)
- Zheng, T.; Qu, K.; Darkwa, J.; Calautit, J.K. Evaluating Urban Heat Island Mitigation Strategies for a Subtropical City Centre (a Case Study in Osaka, Japan). *Energy* **2022**, *250*, 123721. [\[CrossRef\]](#)
- Alsaad, H.; Hartmann, M.; Hilbel, R.; Voelker, C. ENVI-Met Validation Data Accompanied with Simulation Data of the Impact of Facade Greening on the Urban Microclimate. *Data Brief* **2022**, *42*, 108200. [\[CrossRef\]](#)

21. Liu, Z.; Cheng, W.; Jim, C.Y.; Morakinyo, T.E.; Shi, Y.; Ng, E. Heat Mitigation Benefits of Urban Green and Blue Infrastructures: A Systematic Review of Modeling Techniques, Validation and Scenario Simulation in ENVI-Met V4. *Build. Environ.* **2021**, *200*, 107939. [CrossRef]
22. Liu, Q.; Wen, J.; Qu, Y.; He, T.; Zhang, X. Broadband Albedo. In *Advanced Remote Sensing: Terrestrial Information Extraction and Applications*; Liang, S., Wang, J., Li, X., Eds.; Academic Press: San Diego, CA, USA, 2013.
23. Gui, J.; Phelan, P.; Kaloush, K.; Golden, J. Impact of Pavement Thermophysical Properties on Surface Temperatures. *J. Mater. Civ. Eng.* **2007**, *19*, 683–690. [CrossRef]
24. Wayne Lee, K.; Kohm, S. Cool Pavements as Sustainable Approaches for Green Streets and Highways. *Green Energy Technol.* **2014**, *204*, 439–453.
25. Squires, S.W.; Veverka, J. Variation of Albedo with Solar Incidence Angle on Planetary Surfaces. *Icarus* **1982**, *50*, 115–122. [CrossRef]
26. Di Maria, V.; Rahman, M.; Collins, P.; Dondi, G.; Sangiorgi, C. Urban Heat Island Effect: Thermal Response from Different Types of Exposed Paved Surfaces. *Int. J. Pavement Res. Technol.* **2013**, *6*, 414.
27. Yang, J.; Wang, Z.H.; Kaloush, K.E.; Dylla, H. Effect of Pavement Thermal Properties on Mitigating Urban Heat Islands: A Multi-Scale Modeling Case Study in Phoenix. *Build. Environ.* **2016**, *108*, 110–121. [CrossRef]
28. Aletba, S.R.O.; Abdul Hassan, N.; Putra Jaya, R.; Aminudin, E.; Mahmud, M.Z.H.; Mohamed, A.; Hussein, A.A. Thermal Performance of Cooling Strategies for Asphalt Pavement: A State-of-the-Art Review. *J. Traffic Transp. Eng.* **2021**, *8*, 356–373. [CrossRef]
29. O'Malley, C.; Kikumoto, H. An Investigation into Heat Storage by Adopting Local Climate Zones and Nocturnal-Diurnal Urban Heat Island Differences in the Tokyo Prefecture. *Sustain. Cities Soc.* **2022**, *83*, 103959. [CrossRef]
30. Moretti, L.; Di Mascio, P.; Fusco, C. Porous concrete for pedestrian pavements. *Water* **2019**, *11*, 2105. [CrossRef]
31. Moretti, L.; Loprencipe, G. Climate Change and Transport Infrastructures: State of the Art. *Sustainability* **2018**, *10*, 4098. [CrossRef]
32. Nwakaire, C.M.; Onn, C.C.; Yap, S.P.; Yuen, C.W.; Onodagu, P.D. Urban Heat Island Studies with Emphasis on Urban Pavements: A Review. *Sustain. Cities Soc.* **2020**, *63*, 102476. [CrossRef]
33. Moretti, L.; Cantisani, G.; Carpiceci, M.; D'andrea, A.; Del Serrone, G.; Di Mascio, P.; Loprencipe, G. Effect of Sampietrini Pavers on Urban Heat Islands. *Int. J. Environ. Res. Public Health* **2021**, *18*, 13108. [CrossRef]
34. Abdulateef, M.F.; Al-Alwan, A.S.H. The Effectiveness of Urban Green Infrastructure in Reducing Surface Urban Heat Island. *Ain Shams Eng. J.* **2021**, *13*, 101526. [CrossRef]
35. Fahed, J.; Kinab, E.; Ginestet, S.; Adolphe, L. Impact of Urban Heat Island Mitigation Measures on Microclimate and Pedestrian Comfort in a Dense Urban District of Lebanon. *Sustain. Cities Soc.* **2020**, *61*, 102375. [CrossRef]
36. Levinson, R.; Akbari, H. *Effects of Composition and Exposure on the Solar Reflectance of Portland Cement Concrete*; Elsevier: Amsterdam, The Netherlands, 2002; Volume 32. [CrossRef]
37. UNI EN ISO 7730:2006; Ergonomia Degli Ambienti Termici-Determinazione Analitica e Interpretazione Del Benessere Termico Mediante Il Calcolo Degli Indici PMV e PPD e Dei Criteri di Benessere Termico Locale. UNI (Ente Italiano di Normazione): Milano, Italy, 2006.
38. Humphreys, M.A.; Fergus Nicol, J. The Validity of ISO-PMV for Predicting Comfort Votes in Every-Day Thermal Environments. *Energy Build.* **2002**, *34*, 667–684. [CrossRef]
39. Fanger, P. *Thermal Comfort: Analysis and Applications in Environmental Engineering*; McGraw-Hill: New York, NY, USA, 1972.
40. ASHRAE Standard 55-2017; Thermal Environmental Conditions for Human Occupancy. ASHRAE: Atlanta, GA, USA, 2017.
41. Alfano, G.; Cannistraro, G.; D'Ambrosio, F.R.; Rizzo, G. Notes on the Use of the Tables of Standard ISO 7730 for the Evaluation of the PMV Index. *Indoor Built Environ.* **1996**, *5*, 355–357. [CrossRef]
42. Lau, K.K.L.; Lindberg, F.; Rayner, D.; Thorsson, S. The Effect of Urban Geometry on Mean Radiant Temperature under Future Climate Change: A Study of Three European Cities. *Int. J. Biometeorol.* **2015**, *59*, 799–814. [CrossRef]
43. Liu, K.; You, W.; Chen, X.; Liu, W. Study on the Influence of Globe Thermometer Method on the Accuracy of Calculating Outdoor Mean Radiant Temperature and Thermal Comfort. *Atmosphere* **2022**, *13*, 809. [CrossRef]
44. Luki, M.; Filipovi, D.; Pecelj, M.; Crnogorac, L.; Luki, B.; Divjak, L.; Luki, A.; Vuči, A.; Jänicke, B.; Dzyuban, Y.; et al. Assessment of Outdoor Thermal Comfort in Serbia's Urban Environments during Different Seasons. *Atmosphere* **2021**, *12*, 1084. [CrossRef]
45. d'Ambrosio Alfano, F.R.; Ficco, G.; Frattolillo, A.; Palella, B.I.; Riccio, G. Mean Radiant Temperature Measurements through Small Black Globes under Forced Convection Conditions. *Atmosphere* **2021**, *12*, 621. [CrossRef]
46. Moretti, L.; Cantisani, G.; Carpiceci, M.; D'Andrea, A.; Del Serrone, G.; Di Mascio, P.; Peluso, P.; Loprencipe, G. Investigation of Parking Lot Pavements to Counteract Urban Heat Islands. *Sustainability* **2022**, *14*, 7273. [CrossRef]
47. Che Tempo Faceva a Roma—Archivio Meteo Roma. Available online: <https://www.ilmeteo.it/portale/archivio-meteo/Roma> (accessed on 31 July 2022).
48. Lawrence, E.O.; Pomerantz, M.; Pon, B.; Akbari, H.; Chang, S.-C. *The Effect of Pavements' Temperatures on Air Temperatures in Large Cities*; LNBL-43442; Lawrence Berkeley National Laboratory: Berkeley, CA, USA, 2000.
49. Ortiz, E.; Del Valle, U. *Diseño de una Aplicación Computacional Para el Cálculo de Factor de Visión y Temperatura Media Radiante en Espacios Arquitectónicos*; Universidad del Valle: Cali, Colombia, 2017.
50. Masson, V.; Bonhomme, M.; Salagnac, J.L.; Briottet, X.; Lemonsu, A. Solar Panels Reduce Both Global Warming and Urban Heat Island. *Front. Environ. Sci.* **2014**, *2*, 14. [CrossRef]

51. Tan, C.L.; Wong, N.H.; Jusuf, S.K. Effects of vertical greenery on mean radiant temperature in the tropical urban environment. *Landsc. Urban Plan.* **2014**, *127*, 52–64. [[CrossRef](#)]
52. Noro, M.; Lazzarin, R. Urban Heat Island in Padua, Italy: Simulation Analysis and Mitigation Strategies. *Urban Clim.* **2015**, *14*, 187–196. [[CrossRef](#)]
53. Li, Y.; Song, Y. Optimization of Vegetation Arrangement to Improve Microclimate and Thermal Comfort in an Urban Park. *Int. Rev. Spat. Plan. Sustain. Dev.* **2019**, *7*, 18–30. [[CrossRef](#)]
54. Del Serrone, G.; Peluso, P.; Moretti, L. Evaluation of Microclimate Benefits Due to Cool Pavements and Green Infrastructures on Urban Heat Islands. *Atmosphere* **2022**, *13*, 1586. [[CrossRef](#)]
55. Tan, K.; Qin, Y.; Wang, J. Evaluation of the Properties and Carbon Sequestration Potential of Biochar-Modified Pervious Concrete. *Constr. Build. Mater.* **2022**, *314*, 125648. [[CrossRef](#)]
56. Wang, J.; Meng, Q.; Zou, Y.; Qi, Q.; Tan, K.; Santamouris, M.; He, B.J. Performance Synergism of Pervious Pavement on Stormwater Management and Urban Heat Island Mitigation: A Review of Its Benefits, Key Parameters, and Co-Benefits Approach. *Water Res.* **2022**, *221*, 118755. [[CrossRef](#)]
57. Zhang, G.; He, B.J. Towards Green Roof Implementation: Drivers, Motivations, Barriers and Recommendations. *Urban For. Urban Green.* **2021**, *58*, 126992. [[CrossRef](#)]
58. Zhang, G.; He, B.J.; Dewancker, B.J. The Maintenance of Prefabricated Green Roofs for Preserving Cooling Performance: A Field Measurement in the Subtropical City of Hangzhou, China. *Sustain. Cities Soc.* **2020**, *61*, 102314. [[CrossRef](#)]
59. Quesada, B.; Sánchez, C.; Cañada, J.; Royo, R.; Payá, J. Experimental results and simulation with TRNSYS of a 7.2 kWp grid-connected photovoltaic system. *Appl. Energy* **2011**, *88*, 1772–1783. [[CrossRef](#)]
60. Kim, H.C.; Fthenakis, V.; Choi, J.K.; Turney, D.E. Life Cycle Greenhouse Gas Emissions of Thin-Film Photovoltaic Electricity Generation. *J. Ind. Ecol.* **2012**, *16*, S110–S121. [[CrossRef](#)]
61. ENEA. Available online: <https://www.enea.it/it> (accessed on 28 October 2022).
62. PVGIS Photovoltaic Geographical Information System. Available online: https://joint-research-centre.ec.europa.eu/pvgis-photovoltaic-geographical-information-system_en (accessed on 31 July 2022).
63. Milev, G.; Hastings, A.; Al-Habaibeh, A. The Environmental and Financial Implications of Expanding the Use of Electric Cars—A Case Study of Scotland. *Energy Built Environ.* **2021**, *2*, 204–213. [[CrossRef](#)]
64. Di Mascio, P.; Moretti, L.; Capannolo, A. Concrete block pavements in urban and local roads: Analysis of stress-strain condition and proposal for a catalogue. *J. Traffic Transp. Eng.* **2019**, *6*, 557–566. [[CrossRef](#)]
65. Zoccali, P.; Moretti, L.; Mascio, P.D.; Loprencipe, G.; D’Andrea, A.; Bonin, G.; Teltayev, B.; Caro, S. Analysis of natural stone block pavements in urban shared areas. *Case Stud. Constr. Mater.* **2018**, *8*, 498–506. [[CrossRef](#)]